



HAL
open science

Phase transition in hydrophobic weak polyelectrolyte gel utilized for water desalination

Varvara Prokacheva, Oleg Rud, Filip Uhlík, Oleg V. Borisov

► **To cite this version:**

Varvara Prokacheva, Oleg Rud, Filip Uhlík, Oleg V. Borisov. Phase transition in hydrophobic weak polyelectrolyte gel utilized for water desalination. *Desalination*, 2021, 511, pp.115092. 10.1016/j.desal.2021.115092 . hal-03867945

HAL Id: hal-03867945

<https://hal.science/hal-03867945>

Submitted on 13 Mar 2024

HAL is a multi-disciplinary open access archive for the deposit and dissemination of scientific research documents, whether they are published or not. The documents may come from teaching and research institutions in France or abroad, or from public or private research centers.

L'archive ouverte pluridisciplinaire **HAL**, est destinée au dépôt et à la diffusion de documents scientifiques de niveau recherche, publiés ou non, émanant des établissements d'enseignement et de recherche français ou étrangers, des laboratoires publics ou privés.

Phase transition in hydrophobic weak polyelectrolyte gel utilized for water desalination

Varvara M. Prokacheva^a, Oleg V. Rud^{a,b,*}, Filip Uhlík^a, Oleg V. Borisov^{b,c}

^aDepartment of Physical and Macromolecular Chemistry, Faculty of Science, Charles University in Prague, Hlavova 8, Praha 2 128 00, Czech Republic

^bInstitute of Macromolecular Compounds of Russian Academy of Sciences, 199004, Bolshoy pr. 31, Saint-Petersburg, Russia ^cInstitut des Sciences Analytiques et de Physico-Chimie pour l'Environnement et les Matériaux, CNRS, Université de Pau et des Pays de l'Adour UMR 5254, Pau, France

Abstract

By this article, we continue studying weak polyelectrolyte hydrogels and their application as a desalination agent. We modeled the desalination process as a four-step reversible thermodynamic cycle transferring ions from a low salinity solution to a high salinity one. The cycle implies reversibility at any stage, therefore the method can achieve the maximum thermodynamic efficiency, comparable to the reverse osmosis. As a driving force for ions movement, we use the fact that compression of the gel leads to a decrease in the gel ionization degree, and therefore to a release of ions entrapped in the gel. We considered the gel composed of the ionogenic units modified by hydrophobic pendants and showed that this modification may significantly increase the number of transferred ions. This increase is caused by a first-order phase transition originated from an interplay between repulsive electrostatic and attractive steric interactions. The transition happens during hydrogel compression; at certain pressure; the gel collapses abruptly changing its volume almost to that of a dry state and releasing almost all ions collected inside. Employing the phase transition allowed us to model the desalination cycle which transfers a much larger number of ions and works at rather low pressures <10bar.

Keywords: desalination, polyelectrolytes, hydrogels, hydrophobic gel, phase separation, mean-field theory

1. Introduction

Desalination. The lack of freshwater forces developing effective methods for seawater desalination. Nowadays, the biggest part of desalinated water is produced by so called membrane desalination methods, such as reverse osmosis (RO), forward osmosis (FO), and electrodialysis [1]. Their share in the world production of desalinated water is continuously growing, which is caused by the high development potential of these technologies. The main directions of the membrane desalination methods are the development of membrane production technologies, the lowering the energy cost and the suppression of membrane fouling processes [2].

Forward osmosis. Forward osmosis (FO) is one of the most promising emerging desalination technology. The idea of the method lies down in choosing a chemical agent (draw agent) that has a better thermodynamic affinity to water molecules than ions dissolved in salty water. The addition of such an agent to one of the two aqueous solutions,

separated by an osmotic membrane, creates a difference of salt ions osmotic pressure and initiates a water flow in the direction from the feed solution to the draw solution.

The following task of the method is to separate the draw agents from the draw solution gaining the desalinated water. To do it, different and specific properties of draw agents are used [3, 4]. For example, the whole class of draw agents is represented by thermally removable salts [4] (e. g. ammonium carbonate), which decompose by means of heating.

Various smart alternatives to the salt draw agents, such as functionalized magnetic nanoparticles, thermoresponsive polyelectrolyte solutions and stimuli-responsive hydrogels are continuously showing up in literature [5]. All these smart agents are supposed to improve the method in a sense of recycling, cost- and energy-efficiency.

Smart hydrogels. Our current study is dedicated to polyelectrolyte hydrogels. The interest in this topic is justified by the fact that the gel swells in water and retain a significant amount of water inside, whereas the hydrogel particles by themselves do not dissolve in water. At the same time, they exhibit reversible swelling-deswelling changes induced by different stimuli.

The stimuli, which induce the volume changes in the

*Corresponding author

Email address: oleg.rud@natur.cuni.cz (Oleg V. Rud) URL: <http://www.physchem.cz> (Oleg V. Rud)

Preprint submitted to Elsevier

February 8, 2021

gel can be:

1. pH and salinity; for instance, polymethacrylic acid hydrogel undergoes the pH-triggered transition from collapsed

to swollen state. The pH value at which the transition is happening can be shifted by decreasing the solution salinity [6].

2. Solvent composition; polyacrylamide hydrogel undergoes sharp volume phase transition initiated by change of acetone fraction in solution [7, 8].

3. Temperature; the hydrogels consisting N-isopropylacrylamide (NIPAM) at its lower critical solution temperature (LCST) change from hydrophilic to hydrophobic due to the increase in temperature [9, 10, 11]. The same change can be initiated by decrease of temperature upon UCST transition in poly(acrylamide-acrylic acid) hydrogel [12]. Additionally, there are numerous studies related to the phase transition in gels induced by light radiation [13, 14, 15], electric field [16, 17, 18], and magnetic field [19].

Polyelectrolyte hydrogels for desalination. Recently an alternative way of using polyelectrolyte hydrogels for desalination was proposed [20, 21]. The authors of cited studies used the feature of such gels to act simultaneously as draw agents, accumulating water inside, and as osmotic membranes, rejecting salt ions due to the polyelectrolyte properties.

Wilhelm et al. demonstrated how a two-step procedure of swelling and compression of poly(acrylic acid) (PAA) hydrogel can be used for desalinating water [20]. The procedure is the following; initially, the dry gel is immersed in brine. The gel swells reaching the thermodynamic equilibrium between the gel and supernatant phases. At the same time, the ionized monomers of the gel reject the dissolved ions from entering the gel. After swelling the gel is separated from the supernatant and the water, accumulated in the gel particles, is squeezed out using a micro filter supported by a sieve. The extracted solution has a lower salt concentration. The procedure can be repeated afterward by means of the reuse of the hydrogel in subsequent cycles.

As the proof of concept, the hydrogel was compressed up to 80 bar [22]. Although Wilhelm et al. had shown that the same gel can be reused for further cycles, there are several studies proving that the polyacrylic acid hydrogel gets irreversible visible fractures at pressures already below one atmosphere, depending on the solution ionic strength (see, for example, [23, 24]). Therefore, even if the application of high pressure does not break the gel completely, it may significantly limit the number of possible desalination cycles.

Four-step desalination cycle. In our previous work [25] we modeled a four-step fully reversible desalination cycle based on swelling and compression of weak (pH-sensitive) hydrophilic polyelectrolyte gel, similar to PAA. We predicted better efficiency of the four-step cycle compared to that used in [22]. The cycle was free from any thermodynamically irreversible processes like ions or heat dissipation, which guarantees the maximum thermodynamic efficiency. Such efficiency allows the method to compete with the RO desalination in terms of energetic costs. Nevertheless, our model predicted that, pressure needed to

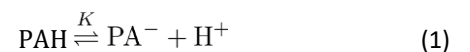
gain a sufficient outcome is of the same order of magnitude as used in [22], about tens of atmospheres, which is also close to that used in RO. This imposes an increased demand on the mechanical parts of the device, therefore the advantage over RO is diminished.

Motivation. The idea motivated the current study is the following: if the ionogenic monomer units of the gel are modified by hydrophobic pendants, the interplay between repulsive electrostatic and hydrophobic interactions will help to decrease the required pressure. The hydrogels made of polymethacrylic acid or polyvinyl amine, as well as already mentioned copolymers containing NIPAM monomers, are good examples of such hydrogels. While their monomer units are charged they exhibit a good affinity to water, whereas being uncharged they are hydrophobic. Thus, in charged state the hydrogel is swollen, and any stimulus affecting the ionization degree, for example, compression, may change dramatically the affinity of the whole hydrogel to solvent and induce the dramatic volume decrease, i. e. collapse. In this study, we predicted the phase transition in such hydrogels and demonstrate how it can be used to improve the water desalination cycle proposed in our previous work [25].

2. Analytical model

Macroscopic hydrogel model. We consider a hydrogel particle in aqueous solution. The particle supposed to be small enough to have sufficiently high surface to volume ratio for better exchanging matter with environment, and, at the same time, sufficiently big to be separated from solution and compressed by a micro filtration membrane (or by a sieve). Thus the size of the particles should be macroscopic, i. e. ranging from microns to millimeters. The assumption of macroscopic size of the gel allows us to construct the model, which disregards the boundary effects due to the electric double layer which size typically ranges from 1 to 100 nm depending on ionic strength of the solution [26].

Thus, we consider the gel as a regular infinite network of polyacid chains, of length N , connected by tetrafunctional cross-links (emulating diamond-like network). Each monomer unit of the hydrogel represents weak acid, which can be ionized according to the following reaction



where PAH and PA^- refer to non-ionized and ionized acidic monomers, respectively. K is the ionization constant.

The gel particle is equilibrated with a bath of aqueous solution of $\text{pH} = 7$, containing monovalent salt ions

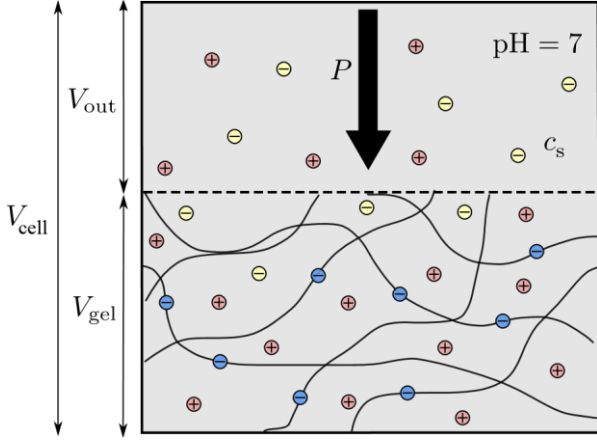


Figure 1: Schematic illustration of the model: polyacid gel is immersed in aqueous solution of monovalent salt and compressed by the pressure P applied to a sieve.

(e.g., NaCl) of concentration c_{Na^+} , and c_{Cl^-} , which approximately equal to the ionic strength of the solution $c_s \approx c_{Na^+} = c_{Cl^-}$.

We assume the uniform extension of the hydrogel chains, which allows relating the end-to-end distance of a single gel strand, R , to an average density of monomer units, c_p .

The volume per one gel chain is therefore

$$V_{gel} = \frac{N}{c_p} = \frac{R^3}{A}, \quad (2)$$

where $A = 3\sqrt{3}/4$ is the coefficient characteristic to the diamond network topology [27].

Mean field theory. Our modeling is based on classical lattice Flory theory of polymers [28]. This approach was employed already many times for studying polyelectrolytes in aqueous solutions [29, 30] and particularly for weak polyelectrolyte hydrogels [31, 32, 33, 25].

Following this approach we write down the free energy of a single chain of the gel as a sum of three independent contributions:

$$F = F_{conf} + F_{int} + F_{ion} \quad (3)$$

which all appear to be density functionals of system components.

The first term in Equation 3 is the conformational free energy of the gel, which models finite extensibility of the network strands

$$[34] \quad \frac{F_{conf}}{k_B T} = \frac{3}{2} \frac{R^2/(b^2 N) - 1}{1 - R^2/(b^2 N^2)} - \frac{3}{2} \ln \left(\frac{R^2}{b^2 N} \right) \quad (4)$$

where b is the linear dimension of a monomer unit, which we set to be the same as of a water molecule, $b = 0.31 \text{ nm}$.

The second term is the contribution of non-electrostatic (steric) interactions [28]

$$\frac{F_{int}}{k_B T} = \frac{N}{c_p} [(1 - c_p) \ln(1 - c_p) - \chi c_p^2] \quad (5)$$

where χ is the Flory-Huggins parameter, which reflects the affinity of polymer to water molecules (i. e., solubility).

In the current study, we consider two cases of hydrogel composed of hydrophilic and hydrophobic units, i. e. $\chi = 0$ and $\chi = 2$ correspondingly. The last case models nearly a hydrogel made of polymethacrylic acid (see Table A.1 in the appendix with calculated χ values for different polymers).

The third term in Equation 3 accounts for ionic contributions. It accounts for the translational entropy of mobile ions and for their partial pressure inside and outside the gel

$$\frac{F_{ion}}{k_B T} = \frac{2c_s N}{c_p} \left[1 - \frac{v}{t} \left(1 + \frac{\alpha c_p}{2c_s} \right)^2 \right] + N \ln(1 - \alpha) \quad (6)$$

where ionization degree, α , is calculated based on local ionization equilibrium and the local electroneutrality condition

$$\xi = \frac{1 - \alpha}{10} = 1 + \frac{\alpha c_p}{2c_s} - \frac{\alpha c_p}{2c_s} \alpha \quad (7)$$

ξ is the Donnan partition coefficient. The derivation of the last two equations can be found in [30, 25].

Equation of state. By substituting Equations 4, 5, 6 to Equation 3, we obtain the equation for the hydrogel free energy as function of gel density and outside salinity, $F = F(c_p, c_s)$. A derivative of this function with respect to volume gives the hydrogel partial pressure, p , i. e. the pressure which needs to be applied to the gel via sieve in order to make its density to be equal to c_p

$$p(c_p, c_s) = - \left(\frac{\partial F(c_p(V_{gel}), c_s)}{\partial V_{gel}} \right)_{c_s} \quad (8)$$

The expanded view of this equation is shown in Appendix Equation B.1.

Open and closed system. The Equation 8 is the equation of state which relates p , c_p and c_s in the situation when the gel

is in equilibrium with a very big (infinite) bath of ionic strength, c_s ; the so-called open system. If the volume of the bath is finite, i. e. in a closed system, the compression of the gel changes the surrounding solution ionic strength. Indeed, the ratio of ion concentrations inside (in) and outside the gel follows the Donnan partitioning law, i. e.

$c_{\text{Na}^+}/c_{\text{Na}^+}^{\text{in}} = c_{\text{Cl}^-}^{\text{in}}/c_{\text{Cl}^-} = \xi$. Roughly speaking, when the strong polyelectrolyte gel is compressed it releases water, whereas the neutralizing counterions remain in gel, which implies that the outside solution gets diluted by extracted from gel water (see Figure 1). Thus the compression of strong polyelectrolyte hydrogel leads to a decrease in the surrounding ionic strength, whereas compression of weak polyelectrolyte hydrogels may increase it due to deionization of polyelectrolyte and associated with it release of counterions [25].

In order to relate p , c_p and c_s in closed system the Equation 8 must be solved together with the restriction of constant number of ions in the cell $N_{\text{const}} = N_+^{\text{out}} + N_+^{\text{in}}$. Thus, for closed system the equation of state of the gel is modified, such that

$$p(c_p, c_s) = - \left(\frac{\partial F(c_p(V_{\text{gel}}), c_s)}{\partial V_{\text{gel}}} \right)_{N_{\text{const}}} \quad (9)$$

given that N_{const} consists of positive ions in the volume V_{out} (see Figure 1), of positive ions compensating the gel charge in gel and of positive ions compensating the negatively charged mobile ions inside the gel:

$$N_{\text{const}} = c_s V_{\text{out}} + \alpha N + V_{\text{gel}} \xi c_s = c_s V_{\text{out}} + V_{\text{gel}} c_s \xi^{-1} \quad (10)$$

Constant pH. According to the reaction Equation 1 the hydrogel deionization implies the consumption of H^+ ions from the solution (or OH^- ions in case of polybasic gel). Therefore the compression of sole polyacidic hydrogel lead to consumption of H^+ ions from the solution and to release of Na^+ ions, i. e. to exchange of H^+ ion by Na^+ ion. In other words the hydrogel compression releases the Na^+ and OH^- ion pair to solution. The same is applicable to polybasic hydrogel, which would release H^+ and Cl^- ion pairs under compression. If both, polybasic and polyacidic hydrogels, are equilibrated with the same solution during compression, and they produce equal amount of H^+ and OH^- ions, then the pH of the solution remains constant all the time, whereas the salinity increases. Hereinafter we will suppose that the polyacidic gel is compressed (or swells) simultaneously with its mirror image polybasic gel, such that they two produce equal amount of H^+ and OH^- ions and pH remains neutral.

3. Phase transition in the gel

Maxwell construction. The pressure volume dependencies calculated by the Equation 8 for hydrophobic gel appear to be in general non-monotonic, such that they resemble a van der Waals loop well known for real gases. The presence of the loop indicates the first-order phase transition caused by an interplay between the repulsive electrostatic and attractive steric interactions in the gel. This phase transition shows up in a step-wise change of the gel volume at certain pressure, p_{tr} , which is calculated by means of Maxwell construction [35] (see the inset to the Figure 2).

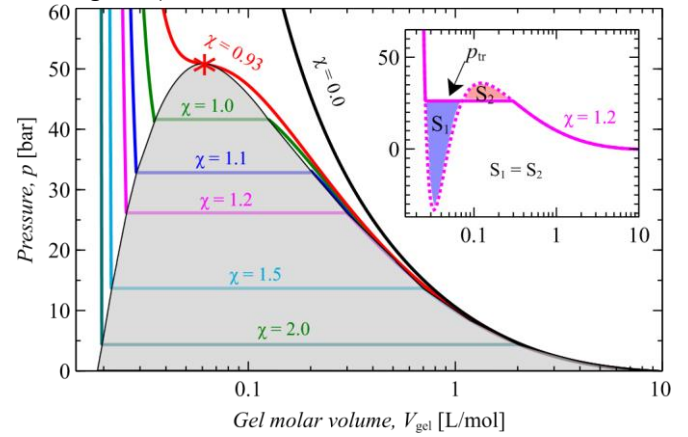


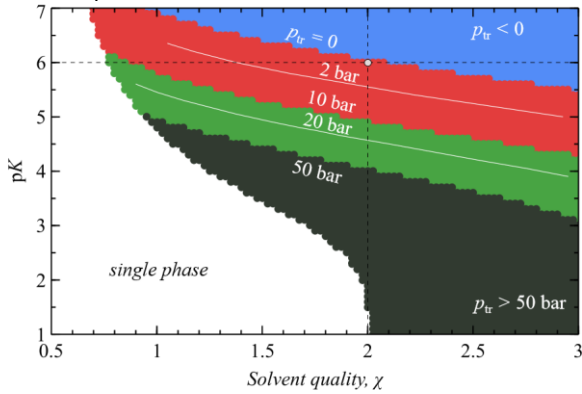
Figure 2: The phase diagram of the polyelectrolyte gel solution with $N = 100$, $pK = 6$ and $c_s = 0.1$ mol/L. The two-phase states area is shown by grey color. The red asterisk corresponds to the critical point. The inset illustrates the Maxwell construction used for calculation of the transition pressure, p_{tr} , for particular gel with $\chi = 1.2$.

Phase transition. Figure 2 represents a set of pressure volume curves calculated for a hydrogel with $N = 100$, $pK = 6$ and with different values of χ , in the bath of salinity $c_s = 0.1$ mol/L. The presented dependencies can be separated to two types: (1) the smoothly increasing with compression, matching the cases when $\chi < 0.93$; and (2) those which have the plateau in the values of pressure, indicating the first-order phase transition happening during compression.

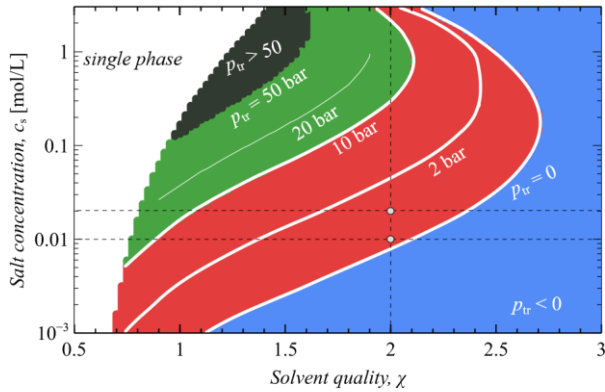
These curves consist of three regions. The slowly decreasing dependency from the right-hand side corresponds to a state when the gel is in single swollen phase; the gel reacts to compression by a smooth increase of its partial pressure. The region where pressure is constant, corresponds to a coexistence of two phases: the phase of swollen gel, which contains a lot of water inside and the phase of collapsed gel, which contains almost no water. At this stage, the compression increases the fraction of the collapsed phase. When the fraction of the swollen phase is depleted, the pressure starts increasing again, and, at this time, the increase is much sharper, which reflects the compression of solid-state gel.

The particular value of pressure, at which the transition is happening, p_{tr} , is different for different pK , χ , and c_s .

Phase diagrams. Figure 3a represents the phase diagram of hydrogel states in $pK\chi$ coordinates for a chosen salinity $c_s = 0.01$ mol/L. The white area on the diagram matches the region, where the gel is in a single swollen state at any compression. The colored regions indicate the presence of phase separation. Black color matches the area where the transition pressure, p_{tr} , is more than 50 bar, green color where p_{tr} is between 10 and 50 bar, and red color between 0 and 10 bar. The blue region corresponds to states when the transition pressure is smaller



(a) $c_s = 0.01$ mol/L



(b) $pK = 6$

Figure 3: Phase diagrams in (a) pK solvent quality χ and (b) salinity c_s solvent quality χ coordinates illustrating the region of two-phase gel. The applied pressure is represented by the color. The black area correspond to $p_{tr} > 50$ bar, green to $10 < p_{tr} \leq 50$ bar, red to $0 \leq p_{tr} \leq 10$ bar and blue to $p_{tr} < 0$ bar.

than zero, i. e. at any positive pressure, the whole gel is present in a single collapsed state; and in order to induce the transition to a swollen state, the gel needs to be stretched.

In the case of $\chi = 2$, only the gel made of very strong polyelectrolyte, $pK < 1.5$, does not experience phase transition at any pressure. The transitionAs the polyelectrolyte gets weaker (pK increases) the phase transition shows up. First, at rather high transition pressure, $p_{tr} > 50$ bar, which gets smaller with further increase of pK . In the case of $pK = 6$, which we consider further, it equals $p_{tr} \approx 0.1$ bar.

Figure 3b is the phase diagram in $c_s\chi$ coordinates for the gel with $pK = 6$. It shows that the transition pressure also depends on the surrounding salinity. As we mentioned already, the gel with $\chi = 2$ equilibrated with solution of salinity $c_s = 0.01$ mol/L experience the phase transition at $p_{tr} \approx 0.1$ bar, whereas in solution of twice bigger salinity $c_s = 0.02$ mol/L the transition pressure is 0.72 bar. Note that the transition pressure changes non monotonically with salinity, which is seen by the bending of constant pressure contour lines on the diagram. In order to better disclose this non-monotonicity of p_{tr} on c_s , we plot a few dependencies of transition pressure on salinity for a set of χ values (see Figure C.8 in Appendix).

In the following section, we will show how the polyelectrolyte gel can be used for transferring ions from low salinity solution to a high salinity one, and how the phase transition happening in hydrophobic gels helps to increase the rate of ion transfer.

4. Desalination cycle

We model the desalination procedure using analogy with the Carnot cycle of reversed heat machine. Such a machine transfers heat from a heat reservoir with low temperature to a reservoir with high temperature. In the desalination cycle ions are transferred from a low salinity solution to a high salinity solution. We compose the cycle from four stages illustrated in Figure 4:

1. the hydrogel is compressed in a closed cell, being in equilibrium with a small amount of solution.
 - At this stage, the outer salinity changes from $c_s^{(1)}$ to $c_s^{(2)}$.
2. Then the compression continues in open system, such that the cell freely exchanges ions with a bath of salinity $c_s^{(2)}$. The bath is assumed to be big enough, such that its salinity does not change, although it exchanges ions with the cell.
3. After compression to a certain volume, the pressure is released allowing the gel to swell in a closed cell; at this stage, the salinity of solution in the cell changes back from $c_s^{(2)}$ to $c_s^{(1)}$.
4. Finally, the gel continue swelling in open system, exchanging the ions with a bath of constant salinity $c_s^{(1)}$, and reaches the initial state.

We modeled all the four processes, using Equations 8 and 9 for two cases of hydrophilic ($\chi = 0$) and hydrophobic ($\chi = 2$) gel.

4.1. Hydrophilic gel

Let us consider a particular desalination cycle, where ions are transferred between two solutions with salinity $c_s^{(1)} = 0.01$ mol/L and $c_s^{(2)} = 0.02$ mol/L and a hydrophilic

weak polyelectrolyte gel is used, so that $\chi = 0$ and $pK = 6$. This cycle is depicted in various coordinates in plots on the left-hand side of Figure 5.

Initially, the gel is equilibrated with the solution of low salinity, $c_s = 0.01$ mol/L and is filling up the volume of the cell $V_{\text{cell}} = V_{\text{gel}}^{\text{init}} \simeq 15$ L/mol. This state is marked by a black circle.

At the first step (blue curve), the cell is isolated from any solution, and the gel is compressed in the cell. The salinity of the outside solution changes from 0.01 to 0.02 mol/L. The number of ions in the cell remains constant during this step (Figure 5c).

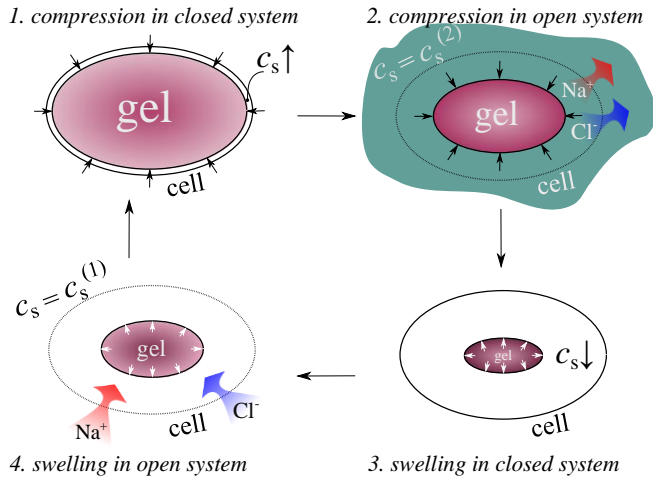


Figure 4: The scheme of the four-step desalination cycle.

Then the cell is put in contact with a big reservoir with solution of the same salinity $c_s = 0.02$ mol/L, and the gel is compressed further (green curve) until applied pressure gets 20 bar. At this stage, the salinity is kept constant, but the number of ions in the cell decreases, which means that they move from the cell to the solution.

At the third step (magenta curve), the cell is isolated again, and the gel swells in equilibrium with the small amount of solution in the cell. The salinity of the outside solution changes back to the initial one (from $c_s = 0.02$ to 0.01 mol/L), whereas the volume of the gel remains smaller than the initial one.

At the last stage (red curve), the cell is connected to a reservoir with salinity $c_s = 0.01$ mol/L and gel reaches the initial state with volume $V_{\text{gel}}^{\text{init}} \simeq 15$ L/mol. At this step, the number of ions increases, which implies that the ions are getting absorbed by the cell from the solution.

In the end, within one cycle about 0.2 ion pairs (calculated per one gel monomer unit) were transferred from the solution of salinity 0.01 mol/L to the solution of salinity 0.02 mol/L.

Since the cycle does not contain any irreversible steps, in terms of energy cost its efficiency appears to be thermodynamically ideal. As a result, the energy expended within one cycle is equal to the number of transferred ion pairs

multiplied by a difference of their chemical potentials in both solutions,

$$W = \Delta N_{\text{Na}^+} \Delta \mu_{\text{Na}^+} + \Delta N_{\text{Cl}^-} \Delta \mu_{\text{Cl}^-} = (\Delta N_{\text{Na}^+} + \Delta N_{\text{Cl}^-}) RT \ln \frac{c_s^{(2)}}{c_s^{(1)}} \quad (1)$$

Thus, the energy needed to transfer one mol of ion pairs approximately equals to 0.26 kJ/mol. The same value can be calculated from the pV cycle as an area enclosed by the four curves.

While composing the cycle, we limited the possible applied pressure by 20 bar, which imposed corresponding restrictions on the possible compression range. It turned out in a limited salinity difference, and in a limited number of transferred ions.

4.2. Hydrophobic gel

Let us consider now a four-step cycle, which uses the same polyelectrolyte gel with the only difference that the Flory-Huggins parameter value is set to $\chi = 2$. The cycle is presented in plots on the right-hand side of Figure 5.

We start from the same initial state as it was for hydrophilic gel. At the first step, the cell is isolated from the solution, and the gel is compressed to the same volume as it was compressed in the previous cycle. Therefore, the change of salinity is the same, so it rises from 0.01 to 0.02 mol/L.

At the second step, the compression continues in open system, so the cell is equilibrated with the reservoir of salinity $c_s = 0.02$ mol/L. At this step, the hydrogel undergoes phase transition and pressure does not change during compression. While the pressure remains the same, compression of the gel makes the fraction of the collapsed phase bigger until the whole gel gets collapsed. At this stage, the gel gets almost completely discharged, therefore all the entrapped co- and counterions leave the cell. Note, the value of pressure remains small and equal to 0.72 bar, so that the state of fully collapsed gel in this case is reached easily. The volume of the gel decreases to ~ 0.02 L/mol, which is about 10 times smaller than it was in the previous cycle. In the previous cycle the volume of the compressed state was about 0.3 L/mol and it required more than 20 times bigger pressure (20 bar).

Then the cell gets isolated and the applied pressure is gradually weakened allowing the gel to swell. The swelling of the gel affects the outside solution, which changes back to the value $c_s = 0.01$ mol/L.

Finally, the cell is equilibrated with the first reservoir. The gel continues swelling, thus the fraction of the collapsed phase decreases until the gel reaches its initial state, when the only swollen phase presents. At this stage, the pressure again remains constant and equal to the initial one, 0.1 bar.

At the end of the cycle, $\Delta N_{\text{Na}^+} = 0.35$ of ion pairs (per gel monomer) were transferred, compared to 0.2 for hydrophilic gel. The reason for such difference lies only in the limitation of

possible applied pressure. If one had compressed the hydrophilic gel to the same density, the number of transferred ions would have appeared to be the same. The required applied pressure, in this case, would have reached hundreds of bar.

The particular value ΔN_{Na^+} can be different depending on how to organize the cycle. Namely, from which salinity it starts, and which salinity difference it is supposed to reach. For instance, the cycle working between 0.05 to 0.07 mol/L salinities transfers approximately $\Delta N_{\text{Na}^+} = 0.4$ ion pairs, whereas the cycle working between $c_s = 0.1$ and 0.2 mol/L transfers only 0.2 ion pairs (see the right column plots in Figures [D.9](#) and [D.10](#) in Appendix). Note that

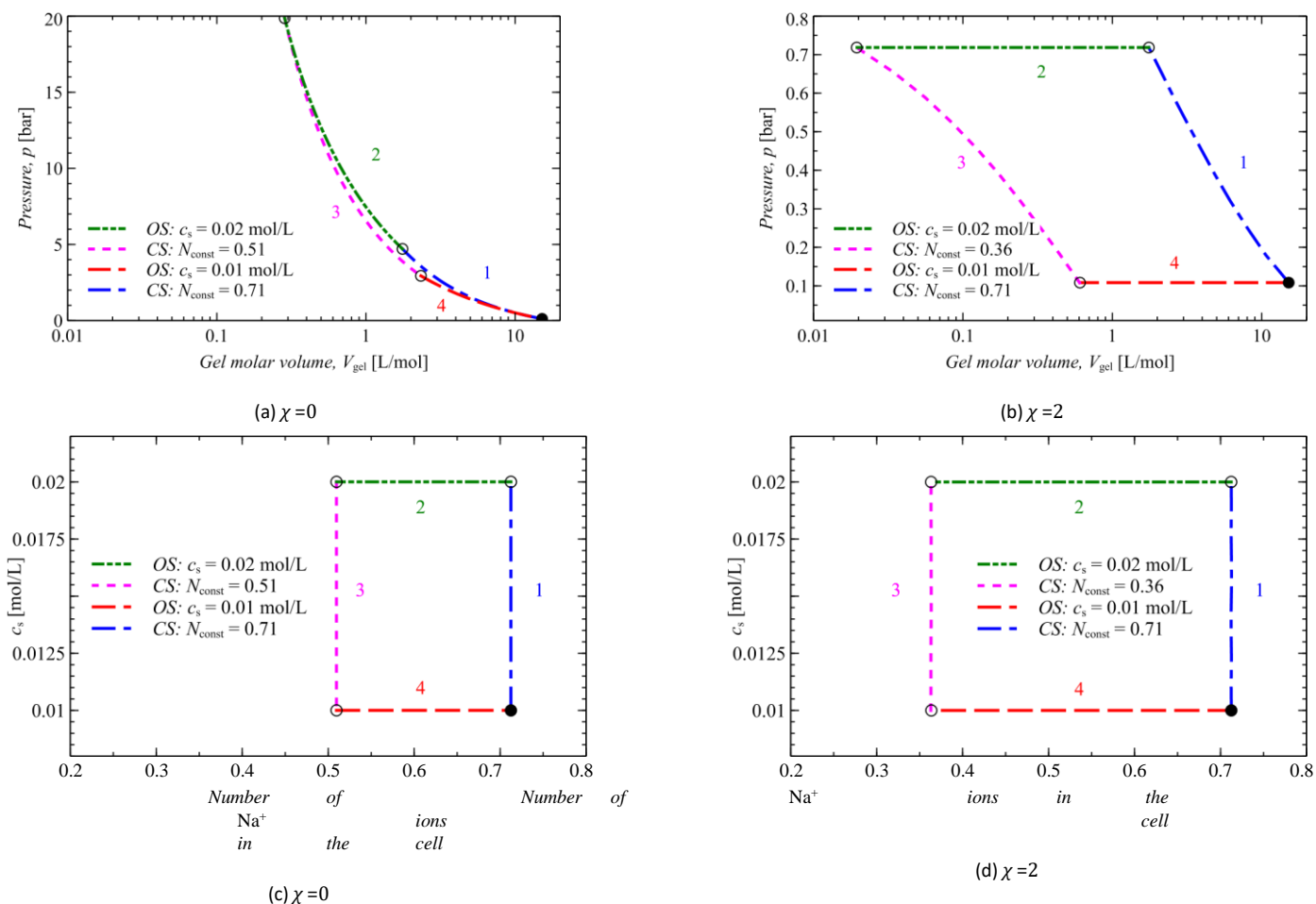
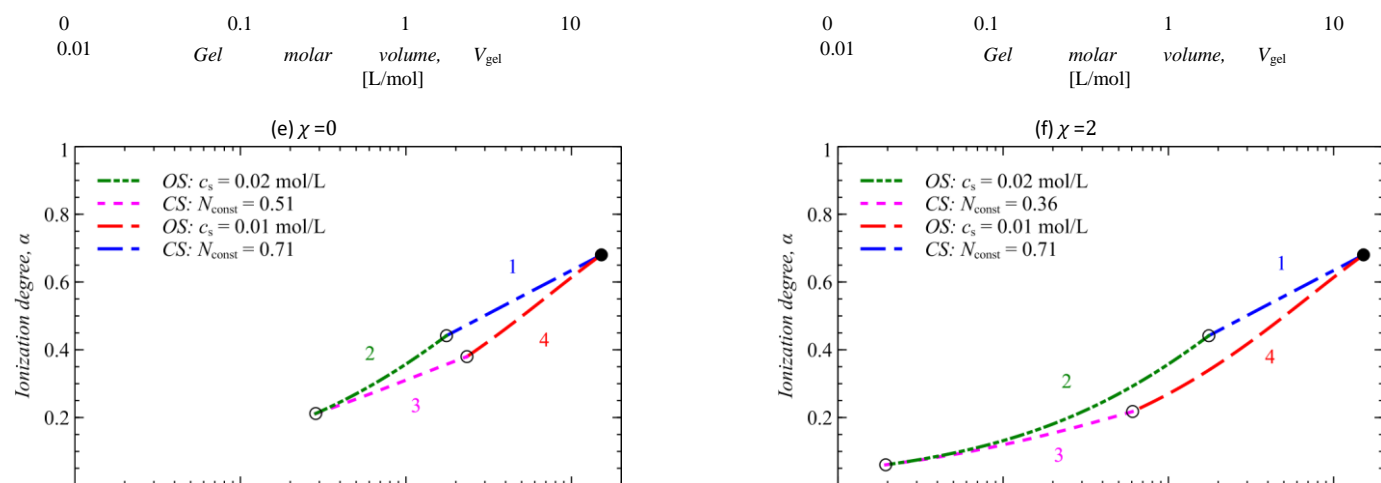


Figure 5: The desalination cycles for weak polyelectrolyte gel at low salinity. The gel has $pK=6$ and $N=100$. The number of ions in the cell is calculated per one monomer of gel. Red and green curves correspond to the regime of the gel in the open system, while the blue and magenta ones represent the gel in the closed system.



in all cases the hydrophilic hydrogels are able to transfer much smaller amounts of ions due to the applied pressure limitation, $p < 20$ bar (see the left columns of referenced Figures).

So, in contrast to the hydrophilic gel, we were able to compress the hydrophobic gel almost to its dry state size, making it almost completely discharged, and thus releasing all the internal solution together with the gel counterions. While the applied pressure was not higher than 0.72 bar.

Conclusions

We studied the use of hydrophobic weak polyelectrolyte hydrogels for water desalination from the thermodynamic point of view. Using the mean-field model we demonstrated that the compression of such a gel may initiate the phase transition showing up in a step-wise change of the gel density. The change of the gel density is happening at certain constant pressure, the value of which is defined by the solution salinity, and by the gel features, such as pK and χ . We found that the transition pressure increases monotonously with a decrease of the ionization constant and solvent quality, but it changes non-monotonously with an increase of salinity. We modeled a four-step desalination cycle, composed of the hydrogel compression and swelling stages, and transferring ions from a reservoir of low salinity solution to a reservoir of high salinity. We demonstrated that the presence of phase transition in cycle allows to reach much higher compression of the gel without rising pressure too much, and to extract a much bigger amount of solution from the gel. At the same the collapse of the gel is accompanied by its almost complete discharge, allowing all the neutralizing ions to escape from the gel.

Acknowledgements

This research was supported by the Czech Science Foundation (grant 19-17847Y) and the Grant Agency of Charles University (project 676218). Government of Russian Federation, grant number 14.W03.31.0022. Charles University Research Centre program (UNCE 204014 - MathMAC University Centre for Mathematical Modelling, Applied Analysis and Computational Mathematics). Computational resources were supplied by the project "e-Infrastruktura CZ" (e-INFRA LM2018140) provided within the program Projects of Large Research, Development and Innovations Infrastructures.

References

- [1] Joyner Eke, Ahmed Yusuf, Adewale Giwa, and Ahmed Sodiq. The global status of desalination: An assessment of current desalination technologies, plants and capacity. *Desalination*, 495:114633, 2020.
- [2] Haya Nassrullah, Shaheen Fatima Anis, Raed Hashaikheh, and Nidal Hilal. Energy for desalination: A state-of-the-art review. *Desalination*, 491:114569, 2020.
- [3] Huayong Luo, Qin Wang, Tian C. Zhang, Tao Tao, Aijiao Zhou, Lin Chen, and Xufeng Bie. A review on the recovery methods of draw solutes in forward osmosis. *Journal of Water Process Engineering*, 4:212 223, 2014.
- [4] Qingchun Ge, Mingming Ling, and Tai-Shung Chung. Draw solutions for forward osmosis processes: Developments, challenges, and prospects for the future. *Journal of Membrane Science*, 442:225 237, 2013.
- [5] Dan Li and Huanting Wang. Smart draw agents for emerging forward osmosis application. *J. Mater. Chem. A*, 1:14049 14060, 2013.
- [6] Jamie Ostroha, Mona Pong, Anthony Lowman, and N Dan. Controlling the collapse/swelling transition in charged hydrogels. 25:4345 4353, 2004.
- [7] Toyochi Tanaka. Collapse of Gels and the Critical Endpoint. *Physical Review Letters*, 40(12):820 823, 1978.
- [8] Michal Ilavsky. Phase transition in swollen gels. 2. effect of charge concentration on the collapse and mechanical behavior of polyacrylamide networks. *Macromolecules*, 15(3):782 788, 1982.
- [9] Dan Li, Xinyi Zhang, Jianfeng Yao, George P. Simon, and Huanting Wang. Stimuli-responsive polymer hydrogels as a new class of draw agent for forward osmosis desalination. *Chem. Commun.*, 47:1710 1712, 2011.
- [10] Shunsuke Hirotsu, Yoshitsugu Hirokawa, and Toyochi Tanaka. Volume-phase transitions of ionized n-isopropylacrylamide gels. *The Journal of Chemical Physics*, 87(2):1392 1395, 1987.
- [11] Xiaobo Hu, Zhen Tong, and L. Andrew Lyon. Synthesis and physicochemical properties of cationic microgels based on poly(N-isopropylmethacrylamide). *Colloid and Polymer Science*, 289(3):333 339, feb 2011.
- [12] Coro Echeverria, Daniel Lopez, and Carmen Mijangos. UCST Responsive Microgels of Poly(acrylamide acrylic acid) Copolymers: Structure and Viscoelastic Properties. *Macromolecules*, 42(22):9118 9123, nov 2009.
- [13] Akira Mamada, Toyochi Tanaka, Dawan Kungwachakun, and Masahiro Irie. Photoinduced Phase Transition of Gels. *Macromolecules*, 23(5):1517 1519, 1990.
- [14] Kun Shi, Zhuang Liu, Yun-Yan Wei, Wei Wang, XiaoJie Ju, Rui Xie, and Liang-Yin Chu. Near-infrared light-responsive poly(n-isopropylacrylamide)/graphene oxide nanocomposite hydrogels with ultrahigh tensibility. *ACS Applied Materials & Interfaces*, 7(49):27289 27298, 2015. PMID: 26580856.
- [15] Atsushi Suzuki and Toyochi Tanaka. Phase transition in polymer gels induced by visible light. *Nature*, 346(6282):345 347, 1990.
- [16] J. P. Gong, T. Nitta, and Y. Osada. Electrokinetic modeling of the contractile phenomena of polyelectrolyte gels. onedimensional capillary model. *The Journal of Physical Chemistry*, 98(38):9583 9587, 1994.
- [17] Huayong Luo, Kelin Wu, Qin Wang, Tian C. Zhang, Hanxing Lu, Hongwei Rong, and Qian Fang. Forward osmosis with electro-responsive p(amps-co-am) hydrogels as draw agents for desalination. *Journal of Membrane Science*, 593:117406, 2020.
- [18] Olga Mergel, Patrick W nemann, Ulrich Simon, Alexander B ker, and Felix A. Plamper. Microgel Size Modulation by Electrochemical Switching. *Chemistry of Materials*, 27(21):7306 7312, 2015.
- [19] Amir Razmjou, Mohammad Reza Barati, George P. Simon, Kiyonori Suzuki, and Huanting Wang. Fast deswelling of nanocomposite polymer hydrogels via magnetic field-induced heating for emerging FO desalination. *Environmental Science and Technology*, 47(12):6297 6305, 2013.
- [20] Johannes H pfnner, Christopher Klein, and Manfred Wilhelm. A novel approach for the desalination of seawater by means of reusable poly(acrylic acid) hydrogels and mechanical force. *Macromolecular Rapid Communications*, 31:1337, 2010.
- [21] Xiuping Zhu, Wulin Yang, Marta C. Hatzell, and Bruce E. Logan. Energy recovery from solutions with different salinities based on swelling and shrinking of hydrogels. *Environmental Science & Technology*, 48(12):7157 7163, 2014. PMID: 24863559.
- [22] Lukas Arens, Julius B. Albrecht, Johannes H pfnner, Karin Schlag, Axel Habicht, Sebastian Seiert, and Manfred Wilhelm. Energy consumption for the desalination of salt water using polyelectrolyte hydrogels as the

separation agent. *Macromolecular Chemistry and Physics*, 218(24):1700237, Nov 2017.

[23] Sylvie Vervoort, Stanislav Patlazhan, Jan Weyts, and Tatiana Budtova. Solvent release from highly swollen gels under compression. *Polymer*, 46(1):121-127, jan 2005.

[24] Xinrui Zhao, Xindi Sun, Jihong Zhang, and Baojun Bai. Gel composition and brine concentration effect on hydrogel dehydration subjected to uniaxial compression. *Journal of Petroleum Science and Engineering*, 182:106358, nov 2019.

[25] Oleg Rud, Oleg Borisov, and Peter Kofovan. Thermodynamic model for a reversible desalination cycle using weak polyelectrolyte hydrogels. *Desalination*, 442:32-43, 2018.

[26] Donald H Napper. *Polymeric stabilization of colloidal dispersions*, volume 3. Academic Pr, 1983.

[27] H. Ibach and H. L th. *Solid-State Physics: An Introduction to Principles of Materials Science*. Advanced texts in physics. Springer Berlin Heidelberg, 2009.

[28] Michael Rubinstein and Ralph H. Colby. *Polymer Physics*. Oxford University Press, Oxford, UK, 2003.

[29] E. B. Zhulina and O. V. Borisov. Self-Assembly in Solution of Block Copolymers with Annealing Polyelectrolyte Blocks. *Macromolecules*, 35(24):9191-9203, nov 2002.

[30] Oleg V. Borisov, Ekaterina B. Zhulina, Frans A. M. Leermakers, Matthias Ballau, and Axel H. E. Mller. Conformations and Solution Properties of Star-Branched Polyelectrolytes. In *Advances in Polymer Science*, volume 241, pages 1-55. 2010.

[31] A. Katchalsky and I. Michaeli. Polyelectrolyte gels in salt solutions. *J. Polym. Sci.*, 15:69, 1955.

[32] E. Yu. Kramarenko, O. E. Philippova, and A. R. Khokhlov. Polyelectrolyte networks as highly sensitive polymers. *Polymer Science Series C*, 48(1):1-20, jul 2006.

[33] Alexey A. Polotsky, Felix A. Plamper, and Oleg V. Borisov. Collapse-to-swelling transitions in pH- and thermoresponsive microgels in aqueous dispersions: The thermodynamic theory. *Macromolecules*, 46(21):8702-8709, 2013.

[34] Bing Miao, Thomas A. Vilgis, Stefanie Poggendorf, and Gabriele Sadowski. Effect of finite extensibility on the equilibrium chain size. *Macromolecular Theory and Simulations*, 19(7):414-420, 2010.

[35] P. Atkins and J. de Paula. *Atkins' Physical Chemistry*. OUP Oxford, 2010.

[36] Charles M. Hansen. *Hansen Solubility Parameters*. CRC Press, jun 2007.

Todo list

Appendix A. Flory-Huggins parameters.

The Flory-Huggins interaction parameter for particular polymer and solvent can be calculated by means of Hansen solubility parameters [36]

$$\chi \approx \frac{v}{RT} \left((D_1 - D_2)^2 + \frac{1}{4} (P_1 - P_2)^2 + \frac{1}{4} (H_1 - H_2)^2 \right), \quad (\text{A.1})$$

where v is molar volume of solvent molecule, in our case it is water, $v = 18$ mL/mol. D_i , P_i and H_i are corresponding impacts to solubility due to dispersion, polar, and hydrogen interactions, their values together with calculated χ parameter are presented in Table A.1.

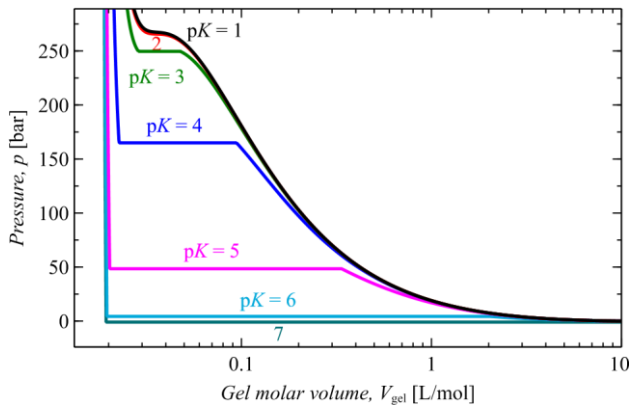
	D	P	H	χ
Methacrylic acid	15.8	2.8	10.2	2.1
Acrylic acid	17.7	6.4	14.9	1.56
Lauril methacrylate	14.4	2.2	5.1	2.87
Vinyl amine	15.7	7.2	11.8	1.83
Water	15.5	16.0	42.3	0

Table A.1: Hansen Solubility Parameters for Selected CompoundsPolymers. D , P , H are in MPa, χ in $k_B T$ [36].

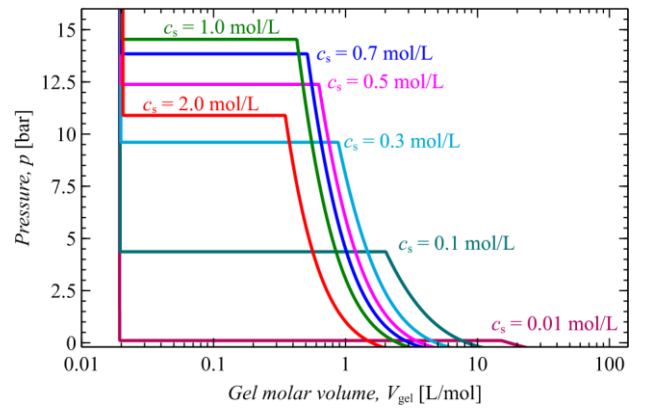
Appendix B. Equation of state.

$$p(c_p(V_{\text{gel}}, c_s)) = - \left(\frac{\partial F(c_p(V_{\text{gel}}, c_s))}{\partial V_{\text{gel}}} \right)_{c_s} = - \frac{A^{2/3} (N c_p)^{5/3} (N-1)}{[N^2 c_p^{2/3} - (AN)^{2/3}]^2} + \frac{c_p}{N} - (\ln(1-c_p) + c_p + \chi c_p^2) - 2c_s \left(1 - \sqrt{1 + \left(\frac{\alpha c_p}{2c_s} \right)^2} \right) \quad (\text{I})$$

Appendix C. Phase diagrams.



(a) $\chi=2$, $c_s=0.1$ mol/L



(b) $\chi=2$, $pK=6$

Figure C.6: The phase diagrams of the polyelectrolyte gel solution.

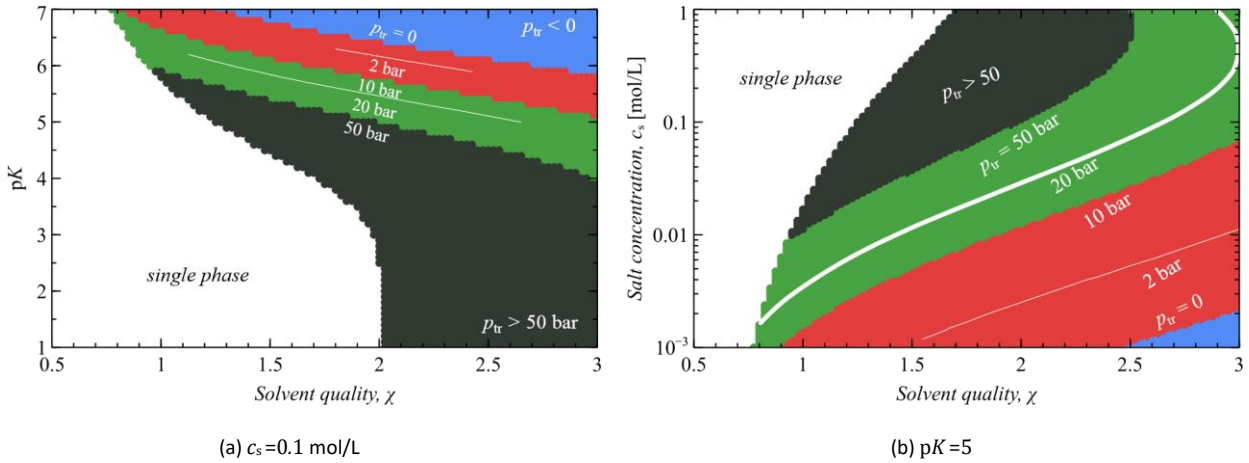


Figure C.7: Phase diagrams in (a) pK solvent quality χ and (b) salinity c_s solvent quality χ coordinates illustrating the region of two-phase gel. The applied pressure is represented by the color. The black symbols correspond to $p > 50 \text{ bar}$, green to $10 < p \leq 50 \text{ bar}$, red to $0 \leq p \leq 10 \text{ bar}$ and blue to $p < 0 \text{ bar}$.

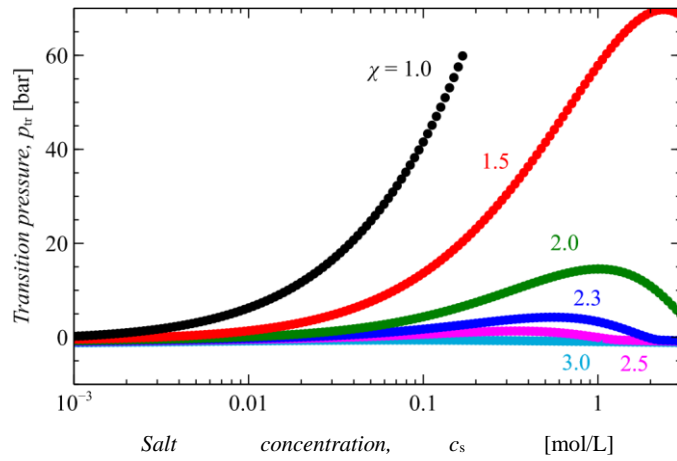
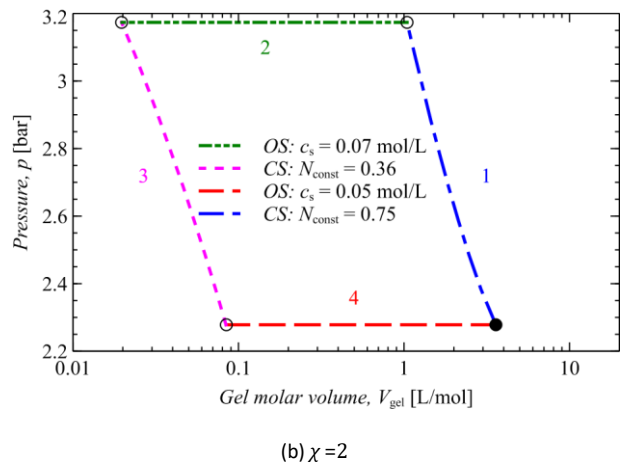
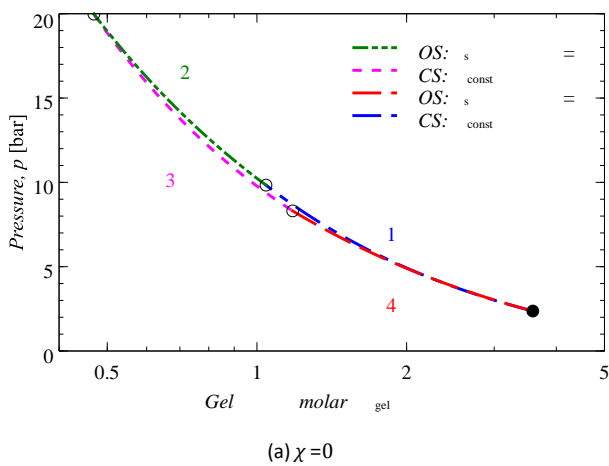


Figure C.8: Dependence of a transition pressure on salinity for different solvent quality χ at $pK = 6$.

Appendix D. Desalination cycles.



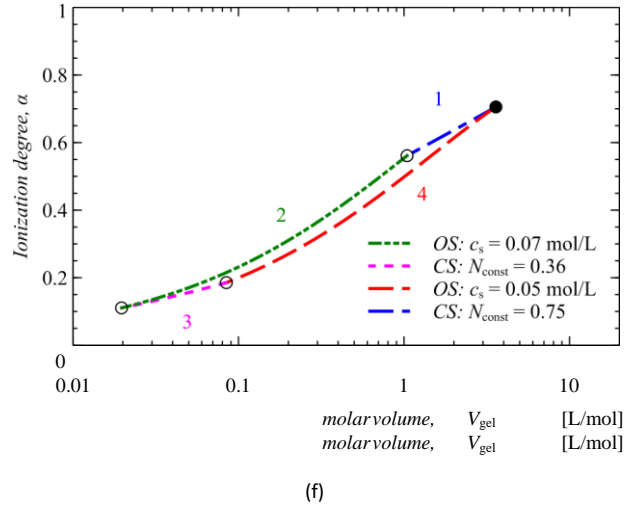
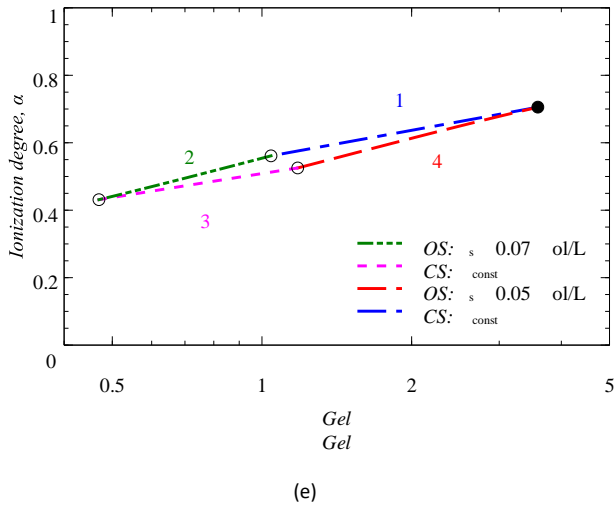
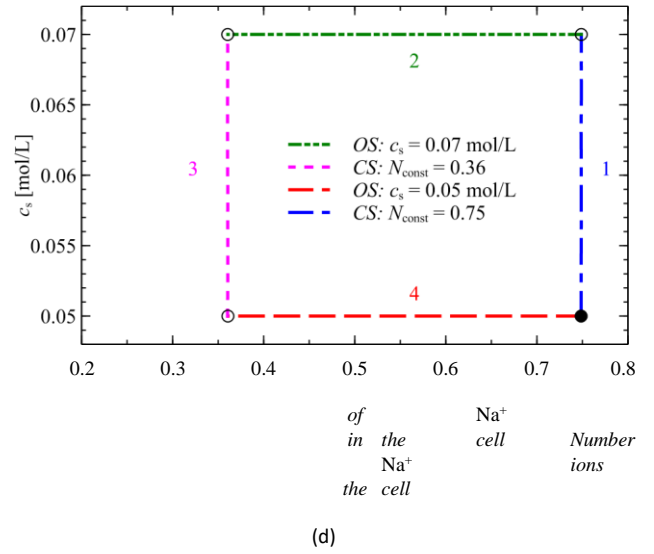
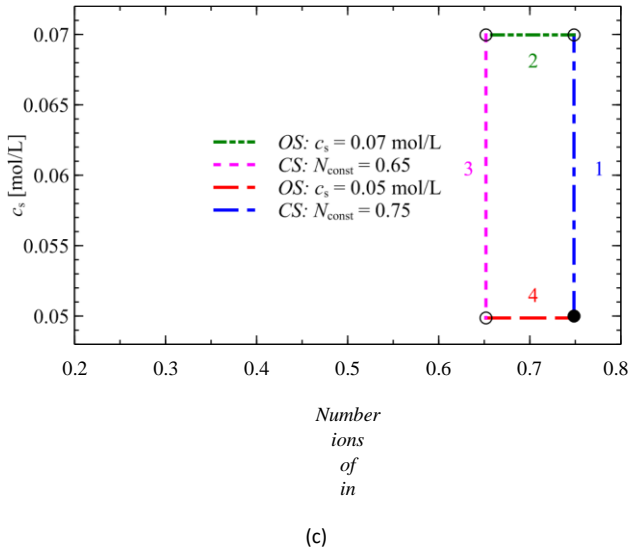
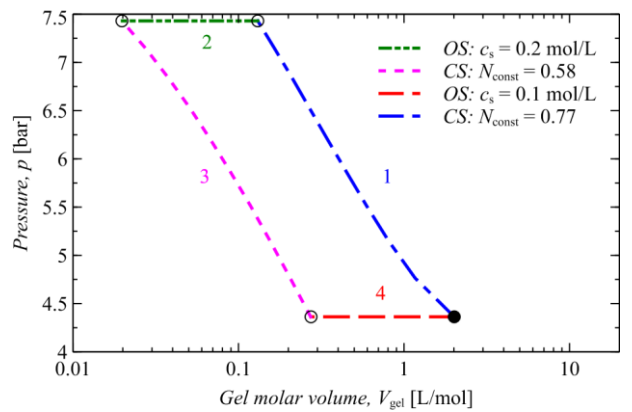
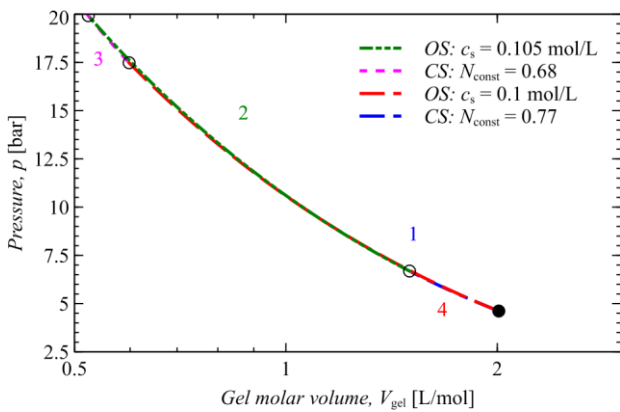
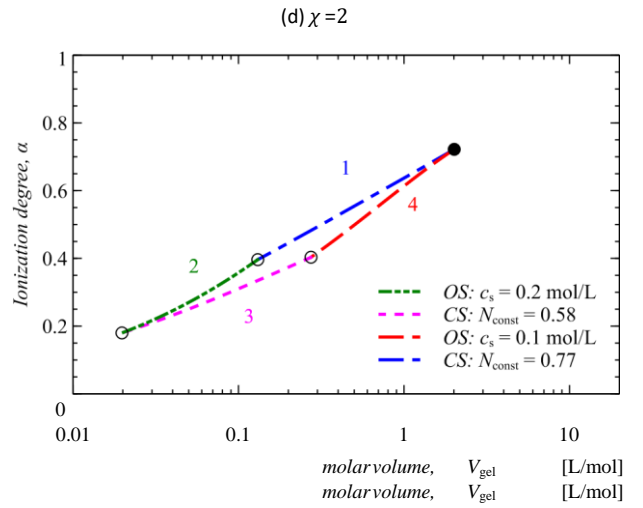
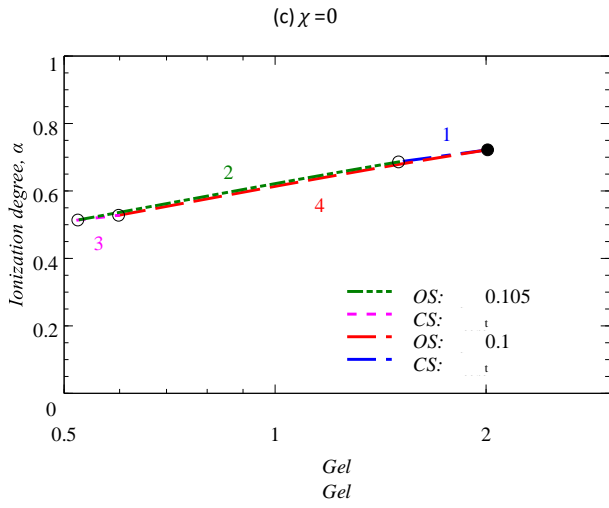
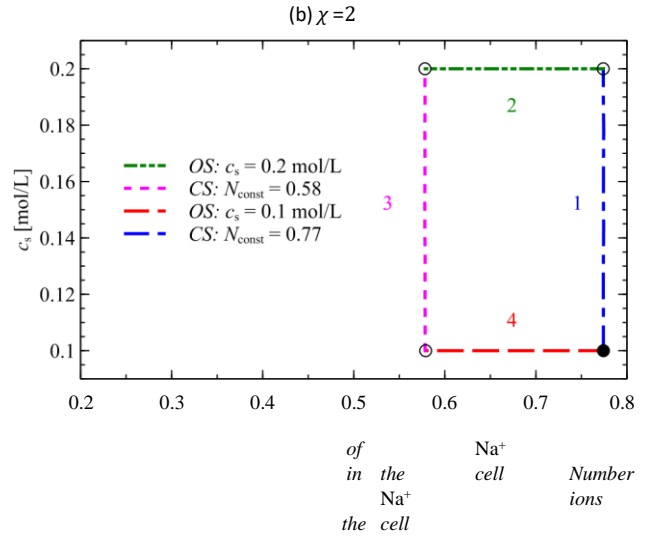
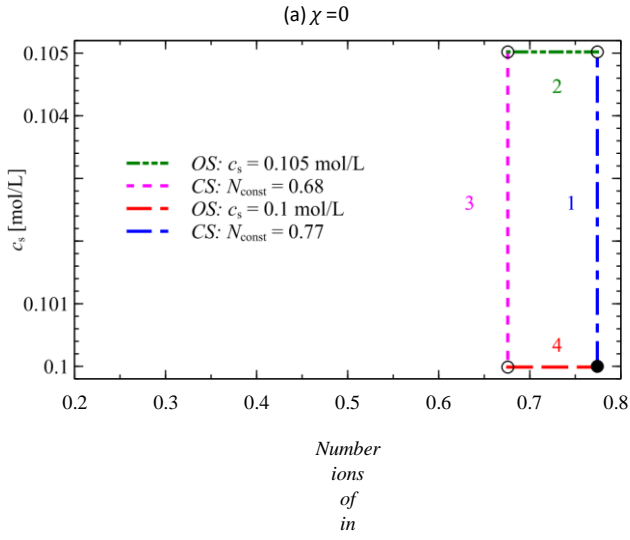


Figure D.9: The desalination cycle for weak polyelectrolyte gel at moderate salinity, $c_s = 0.05$. The gel has $pK = 6$ and $N = 100$. The number of ions in the cell is calculated per one gel monomer. Red and green curves correspond to the regime of the gel in the open system, while the blue and magenta represent the gel in the closed system.





(e)

(f)

Figure D.10: The desalination cycle for weak polyelectrolyte gel with at high salinity, $c_s=0.1$ mol/L. The gel has $pK=6$ and $N=100$. The number of ions in the cell is calculated per one gel monomer. Red and green curves correspond to the regime of the gel in the open system, while the blue and magenta represent the gel in the closed system.